LA-UR -86-2283

CONF-860741--6

MASTER

Los Alamos National Laboratory is operated by the University of California for the United States Department of Energy under contract W-7405-ENG-36

LA-UR--86-2283

RECEIVED

DE86 012419

TITLE NEW RESULTS FOR RARE MUON DECAYS

AUTHOR(S) R. E. Mischke, R. D. Bolton, J. D. Bowman, M. D. Cooper, J. S. Frank, A. L. Hallin, P. A. Heusi, C. M. Hoffman, G. E. Hogan, F. G. Mariam, H. S. Matis, D. E. Nagle, L. E. Piilonen, V. D. Sandberg, G. H. Sanders, U. Sennhau er, R. Werbeck, R. A. Williams, S. L. Wilson, R. Hofstadter, E. B. Hughes, M. W. Ritter, D. Grosnick, S. C. Wright, V. L. Highland, and J. McDonough

SUBMITTED TO Invited Talk for the International Symposium on Weak and Electromagnetic Interactions in Nuclei, Heidelberg, W. Germany, July 1-5, 1986.

DISCLAIMER

Los Alamos National Laboratory
Los Alamos, New Mexico 87545

New Results for Rare Muon Decays

R. E. Mischke, R. D. Bolton, J. D. Bowman, M. D. Cooper, J. S. Frank, A. L. Hallin,[a] P. A. Heusi,[b] C. M. Hoffman, G. E. Hogan, F. G. Mariam, H. S. Matis,[c] D. E. Nagle, L. E. Piilonen, V. D. Sandberg, G. H. Sanders, U. Sennhauser,[d] R. Werbeck, and R. A. Williams
Los Alamos National Laboratory, Los Alamos, NM 87545

S. L. Wilson,[e] R. Hofstadter, E. B. Hughes, and M. W. Ritter[f]
Stanford University, Stanford, CA 94305

D. Grosnick and S. C. Wright
University of Chicago, Chicago, IL 60637

V. L. Highland and J. McDonough
Temple University, Philadelphia, PA 19122

1. Abstract

Branching-ratio limits obtained with the Crystal Box detector are presented for the rare muon decays $\mu \to eee$, $\mu \to e\gamma$, and $\mu \to e\gamma\gamma$. These decays, which violate the conservation of separate lepton-family numbers, are expected to occur in many extensions to the standard model. We found no candidates for the decay $\mu \to eee$, yielding an upper limit for the branching ratio of $B_{\mu 3e} < 3.1 \times 10^{-11}$ (90% C.L.). A maximum-likelihood analysis of the $\mu \to e\gamma$ candidates yields an upper limit of $B_{\mu e\gamma} < 4.9 \times 10^{-11}$ and an analogous analysis of $\mu \to e\gamma\gamma$ candidates gives an upper limit of $B_{\mu e\gamma\gamma} < 7.2 \times 10^{-11}$. These results strengthen the constraints on models that allow transitions between lepton families.

2. Introduction

The muon has been an enigma since its discovery. Originally mistaken for the pion, it behaves as if it were a heavy electron. The only known decay mode of the muon is $\mu \to e\nu_\mu\bar{\nu}_e$ (and its radiative correction). Many experiments have searched for lepton-family-nonconserving decays such as $\mu \to e\gamma$, $\mu \to 3e$, and $\mu \to e\gamma\gamma$. Figure 1 shows how the limits for these decays have been steadily improved. The absence of the decay $\mu \to e\gamma$ led to the discovery of separate muon and electron neutrinos and to the hypothesis of separate conserved quantum numbers for electrons and muons. Recently it has become widely accepted that because lepton number does not relate to a space-time symmetry as do energy and momentum conservation, nor is it associated with a massless gauge boson, as is electric charge, there is no reason to think it is a conserved quantity. The standard model[1] has been very successful but it does not address the question of lepton number. Because the standard model is incomplete, many extensions have been considered and several of these can lead to lepton-family nonconservation.[2] The existing experimental upper limits[3-5] impose model-dependent constraints on the theoretical parameters, like mixing angles or gauge-boson masses, that describe such processes. In general, there are too many free parameters in these theories to predict absolute decay rates. However, they frequently predict the ratios of rates for these decays. It is important for experiments to consider all channels because it is impossible to predict in which decay mode lepton-number nonconservation will first be seen.

---

[a] Present address: Princeton University, Princeton, NJ 08544
[b] Present address: ELEKTROWATT Ing. AG., Zurich, Switzerland
[c] Present address: Lawrence Berkeley Laboratory, Berkeley, CA 94720
[d] Present address: SIN, CH-5234 Villigen, Switzerland
[e] Present address: Los Alamos National Laboratory, Los Alamos, NM 87545
[f] present address: Lockheed Missiles and Space Company, Palo Alto, CA 94304

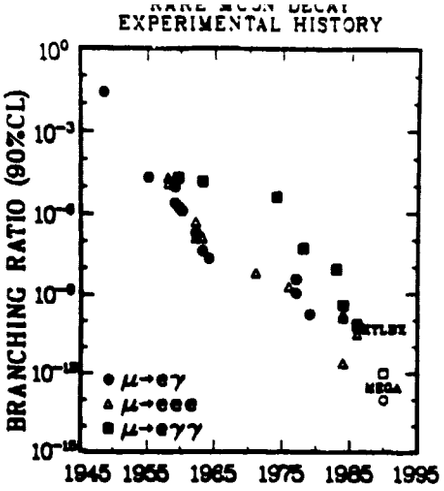

Fig. 1 Branching ratio limits for rare muon decays versus the year of the measurement

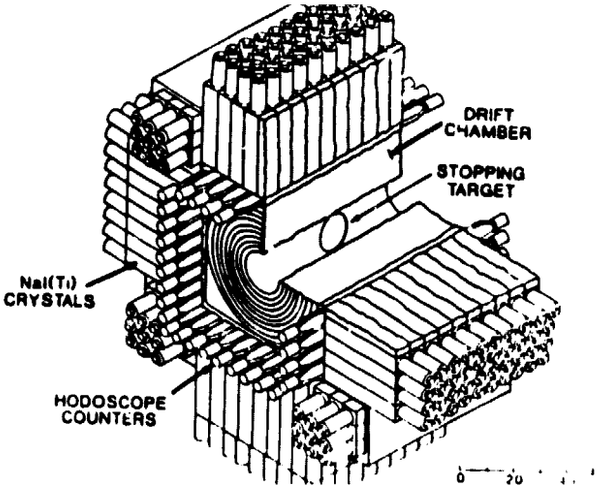

Fig. 2 The Crystal Box detector

3. Detector and Data Acquisition

The Crystal Box detector,[6] shown in Fig. 2, is located at the Stopped Muon Channel of LAMPF. A large (6.7-cm effective radius), thin (52 mg/cm^2) polystyrene target stops 26 MeV/c positive muons. Surrounding the target is a 728-cell, eight-plane, large-stereo-angle drift chamber,[7] which determines the three dimensional trajectories of charged particles. The drift chamber is surrounded by a 36-section plastic scintillator hodoscope, which provides discrimination between charged and neutral particles and timing resolution for charged particles of 290 ps (FWHM). Energy information is provided by a large-solid-angle 396-element NaI(Tl) array. Ninety crystals form each of four quadrants and nine crystals are arranged in each corner between two quadrants. The detector has an energy resolution of ~8% FWHM at 50 MeV for both positrons and photons, and a timing resolution of 1.2 ns for photons. The position resolution of the origin of a charged particle on the target is 2 mm. The photon conversion point is determined to 4.1 cm from energy sharing between NaI crystals.

The absolute gain of each NaI crystal was set to 10% using a Pu-α-Be source (4.43 MeV γ) and calibrated using photons from the reactions $\pi^- p \to n\pi^0$ ($\pi^0 \to \gamma\gamma$) ($55 \lesssim E_\gamma \lesssim 83$ MeV) and $\pi^- p \to n\gamma$ ($E_\gamma = 129.4$ MeV). The pion data were taken with a liquid-hydrogen target replacing the drift chamber. The gain stability of each NaI channel was monitored every two hours using a Xe flashtube and fiber optics cables connected to each photomultiplier and by the end-point of the positron energy distribution from normal μ decay.

The sensitivity limit of a rare μ decay experiment is determined by the number of μ decays examined and by how well the backgrounds are identified or suppressed. The sources of background are random coincidences between positrons from normal μ decay and bremsstrahlung photons, and the prompt processes $\mu \to eee\nu\bar{\nu}$, $\mu \to e\gamma\nu\bar{\nu}$, and $\mu \to e\gamma\gamma\nu\bar{\nu}$. Random coincidences dominate the background for the Crystal Box in all three decay modes. However, for the $e\gamma$ mode the prompt background contributes about 10%. To identify a rare decay event the energy, time, and position resolutions of the detector must be adequate to show that the particles are in time, that the total energy is equal to that of the muon, and that the vector sum of the momenta is zero. In addition, for 3e events, all tracks must have a common origin on the target.

The data acquisition system collected candidates for all three decay modes simultaneously. The trigger defined a "positron quadrant" as a signal in a hodoscope scintillator with more than 5 MeV of energy in a crystal in one of the three rows of crystals directly behind the scintillator within 15 ns of the hodoscope signal. A "photon quadrant" was defined by requiring energy in the NaI

with no scintillator firing within 20 ns in front of it, or in the nearest scintillator in the adjacent two quadrants. The 3e trigger required that there be signals in three non-adjacent plastic scintillators, that the scintillators be in a geometric pattern kinematically consistent with a 3e decay, and that three scintillators fire within 5 ns of each other. The eγ trigger required a coincidence within ±5 ns of a positron in one quadrant and the opposite photon quadrant, and that each have an NaI energy greater than 30 MeV. The $e^+\gamma\gamma$ trigger required a time coincidence within ±12 ns of a positron quadrant and two photon quadrants, with at least 70 MeV deposited in the NaI calorimeter. These trigger requirements generated a trigger rate of about 20 Hz with 7.7 MHz instantaneous of muons stopping in the target at a 7% duty factor (500 kHz average).

The trigger generated a signal to start all the TDC's, a gate for the ADC's, and a start signal for the readout of the event. For each event all the scintillator ADC and TDC data were recorded. Distributed processors performed a sparse data scan for the drift-chamber TDC information and the NaI pulse-height and timing information. In addition, a second ADC with a different gate was used on the NaI crystals to detect pileup. A computer acquired and filtered the events by making on-line cuts before taping the data.

Approximately 10^6-10^7 events were recorded for each trigger from 1.2×10^{12} muons that were stopped. About 30% of the data were taken without benefit of the additional ADC system to reject pileup in the NaI. All the data were processed by a multistage filtering process. The data remaining after the first two passes consisted of 10^3-10^4 events in each of the data streams. These were carefully investigated to look for a prompt signal and any candidates for lepton-family-nonconserving decays.

4. μ → eγ Analysis

The data sample containing possible $\mu \to e\gamma$ events consisted of 17 073 events satisfying $|\Delta t_{e\gamma}| < 5$ ns, $\theta_{e\gamma} \geq 160^\circ$, $E_e \geq 44$ MeV, and $E_\gamma \geq 40$ MeV. An ideal $\mu \to e\gamma$ event would have $|\Delta t_{e\gamma}| = 0$, $\theta_{e\gamma} = 180^\circ$, and $E_e = E_\gamma = 52.8$ MeV. Fig. 3a shows $\Delta t_{e\gamma}$, the photon-positron relative timing, for a subset of these events. The broad distribution is due to random coincidences, while the prompt peak is due to $\mu^+ \to e^+\nu\bar{\nu}\gamma$ and possible $\mu^+ \to e^+\gamma$ events.

The number of each component in the data sample was determined by maximizing the likelihood

$$L(n_{e\gamma}, n_{IB}) = \prod_{i=1}^{N} \left[\frac{n_{e\gamma}}{N} P(\vec{x}_i) + \frac{n_{IB}}{N} Q(\vec{x}_i) + \frac{n_R}{N} R(\vec{x}_i) \right]$$

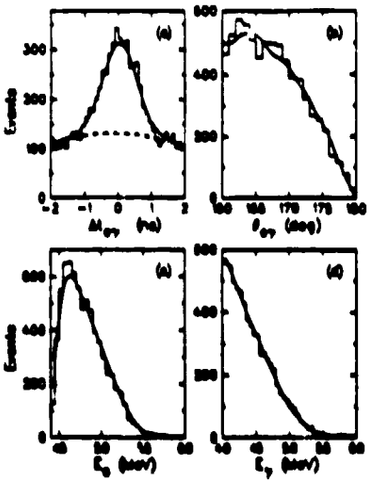

Fig. 3 Spectra for each of the quantities used in the μ → eγ data analysis

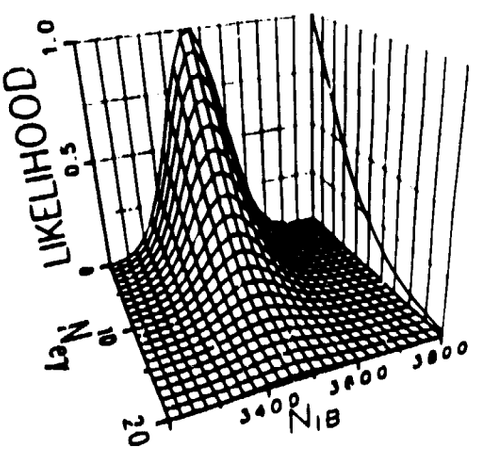

Fig. 4 The likelihood function versus the number of μ → eγ and μ → eγνν̄ in the data

with respect to the parameters $n_{e\gamma}$, n_{IB}, and $n_R = N - n_{e\gamma} - n_{IB}$ that estimated the number of $\mu^+ \to e^+\gamma$, $\mu^+ \to e^+\nu\bar{\nu}\gamma$, and random events in the total sample of N events. The vector $\vec{x}$ had components $\theta_{e\gamma}$, $\Delta t_{e\gamma}$, E_e, and E_γ. P, Q, and R were the probability distributions for $\mu^+ \to e^+\gamma$, $\mu^+ \to e^+\nu\bar{\nu}\gamma$, and random events, respectively. The distributions for P and Q and the acceptance of the apparatus were determined with a Monte Carlo simulation, based on the shower code EGS3,[8] that accurately reproduced the response of the detector to photons and positrons.

Fig. 4 shows the normalized likelihood function. It peaks at $n_{e\gamma} = 0$ and $n_{IB} = 3470 \pm 80 \pm 300$ events. The latter agrees well with the $3960 \pm 90 \pm 200$ $\mu^+ \to e^+\nu\bar{\nu}\gamma$ events expected in the data. The likelihood function distribution implies $n_{e\gamma} < 11$ events (90% C.L.). Using the number of muons stopped, the apparatus acceptance for $\mu^+ \to e^+\gamma$, 0.305, and the detection efficiency, 0.613, we obtain $B_{e\gamma} < 4.9 \times 10^{-11}$. Fig. 3 shows the agreement between the data (histogrammed) and the best mix of $\mu^+ \to e^+\nu\bar{\nu}\gamma$ and randoms (smooth curve) as determined by the likelihood analysis.

5. $\mu \to e\gamma\gamma$ Analysis

The number of events surviving the first analysis from the $e\gamma\gamma$ trigger was 41 656; an additional 968 candidates were found in the $e\gamma$-triggered events, where the positron and one photon occupied the same quadrant. Fig. 5 shows the relative timing distribution for some of these events, the majority being backgrounds from triple random coincidences or two-particle prompt events in random coincidence with a third particle (e.g., $\mu^+ \to e^+\nu\bar{\nu}\gamma + \gamma$). The cuts applied during the data analysis removed most of the double- and triple-random coincidences while retaining most of the $\mu^+ \to e^+\gamma\gamma$ events, making minimal assumptions for the $\mu^+ \to e^+\gamma\gamma$ matrix element.[9] Events with one particle showering and appearing as two hits in the trigger in coincidence with another particle were removed by energy cuts.

The number of $\mu^+ \to e^+\gamma\gamma$ events in the remaining sample of nine events was estimated by maximizing the likelihood

$$L(n_{e\gamma\gamma}) = \prod_{i=1}^{N} \left[\frac{n_{e\gamma\gamma}}{N} P(\vec{x}_i) + \frac{n_R}{N} R(\vec{x}_i) \right]$$

with respect to the parameters $n_{e\gamma\gamma}$ and $n_R = N - n_{e\gamma\gamma}$ that estimated the number of $\mu^+ \to e^+\gamma\gamma$ and background events in the sample of N events. The components of $\vec{x}$ were E_{tot}, $\tau = 2t_e - t_{\gamma 1} - t_{\gamma 2}$, $p_\perp = |\vec{p}_a + \vec{p}_b + \vec{p}_c \times \hat{p}_{ab}|$ and $\cos\alpha = \hat{p}_c \cdot \hat{p}_{ab}$, where $\vec{p}_a$ and $\vec{p}_b$ were the momenta most nearly perpendicular to each other, $\hat{p}_{ab}$ was the unit vector normal to the p_a-p_b plane, and $\vec{p}_c$ was the third particle's momentum. P and R were the probability distributions for $\mu^+ \to e^+\gamma\gamma$ and background, respectively. The Monte Carlo program gave the distributions for P and the distributions for R were taken from data with $\tau \neq 0$.

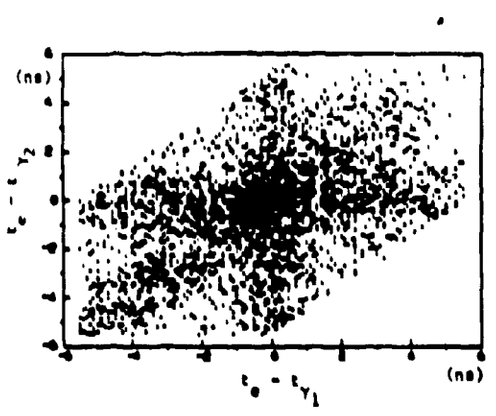

Fig. 5 Timing scatter plot for $\mu \to e\gamma\gamma$ data

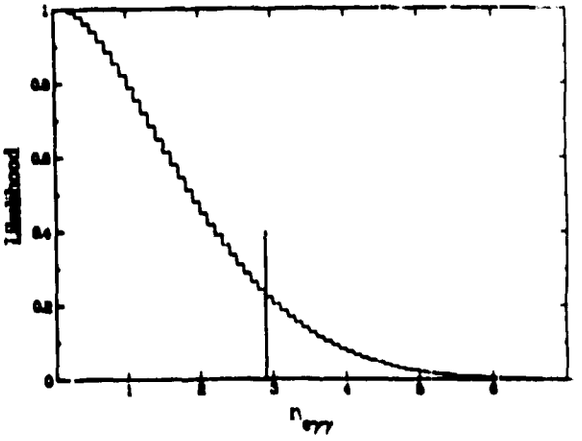

Fig. 6 Maximum likelihood for $\mu \to e\gamma\gamma$ candidates

The likelihood function distribution in Fig. 6 implies $n_{e\gamma\gamma} < 2.9$ (90% C.L.). Using the number of muons stopped, the apparatus acceptance for $\mu^+ \to e^+\gamma\gamma$, 0.064, and the detector efficiency, 0.524, we obtain $B_{e\gamma\gamma} < 7.2 \times 10^{-11}$ (90% C.L.).

6. Summary

The results of the experiment for the three decay modes are as follows:

$$\frac{\Gamma(\mu\to e\gamma)}{\Gamma(\mu\to e\nu\bar{\nu})} < 4.9 \times 10^{-11} \qquad \frac{\Gamma(\mu\to eee)}{\Gamma(\mu\to e\nu\bar{\nu})} < 3.1 \times 10^{-11} \qquad \frac{\Gamma(\mu\to e\gamma\gamma)}{\Gamma(\mu\to e\nu\bar{\nu})} < 7.2 \times 10^{-11}$$

We conclude that there is no evidence for nonconservation of lepton family number. As examples of theoretical constraints imposed by our result, we show how these new values of $B_{\mu e\gamma}$ and $B_{\mu e\gamma\gamma}$ limit the parameters in a few models. Using the formula of Tomozawa[10] for the mass of the constituents of muons and electrons, where the muon is taken to be a 2S excited state of the electron, $B_{\mu e\gamma}$ can be combined with $B_{\mu e\gamma\gamma}$ to yield a lower limit on the mass of the constituents of 7.15×10^7 GeV. In a composite model[11] based on the inclusion of heavy vector weak isodoublets, $\mu \to e\gamma$ constrains the mass scale of the heavy leptons to be $\Lambda > 2.4 \times 10^2$ TeV. In supersymmetric theories,[12] where the symmetry is broken by gravity,[13] the mass of the supersymmetric partner of the muon must be greater than 36 GeV. A model[14] based on O(18) that contains the standard model and a discrete family symmetry with four generations includes massive neutrinos with mass less than 40 GeV. Taking the estimate that the mixing angle with e and μ is $|\theta^*_\mu \theta_e| = 10^{-3}$, the limit on $\mu \to e\gamma$ constrains the neutrino mass to be at the upper end of its range: $M_N > 40$ GeV. An effective Lagrangian analysis of possible deviations from the standard model shows that unless there are unnatural suppressions, $\mu \to e\gamma$ provides a stringent limit on the scale of new interactions of $\Lambda = 10^4$ TeV.[15] In all cases, the mass limits vary as $[B_{\mu e\gamma}]^{-1/4}$.

We acknowledge the extraordinary assistance from the many people at each of our institutions and from the operations staff at LAMPF. This work was supported in part by the U.S. Department of Energy and the National Science Foundation.

7. References

1. S. L. Glashow, Nucl. Phys. 22, 579 (1961); A. Salam, in Elementary Particle Theory: Relativistic Groups and Analyticity (Nobel Symposium No. 8), edited by N. Svartholm (Almqvist and Wiksell, Stockholm, 1968), p. 367; S. Weinberg, Phys. Rev. Lett. 19, 1264 (1967).
2. C.M. Hoffman, in Fundamental Interactions in Low-Energy Systems, ed. P. Dalpiaz et al., (Plenum Press, New York, 1985), p. 138; R. Engfer and H. K. Walter, Ann. Rev. Nucl. Sci. (to be published).
3. W. W. Kinnison et al., Phys. Rev. D 25, 2846 (1982)
4. W. Bertl et al., Phys. Lett. 140B, 299 (1984).
5. G. Azuelos et al., Phys. Rev. Lett. 51, 164 (1983).
6. R.D. Bolton et al., Phys. Rev. Lett. 56, 2461 (1986) and references therein.
7. R.D. Bolton et al., Nucl. Instr. and Methods 241, 52 (1985).
8. R.L. Ford and W.R. Nelson, Stanford Linear Accelerator Center No. SLAC-210, 1978 (unpublished).
9. J. Dreitlein and H. Primakoff, Phys. Rev. 126, 3 5 (1962).
10. Y. Tomozawa, Phys. Rev. D25, 1448 (1982).
11. P. Esposito, Universitá "La Sapienza" - Roma Preprint N. 479, Nov. 1985 (unpublished).
12. J. Ellis and D. V. Nanopoulos, Phys. Lett. 110B, 41 (1983).
13. E. Cremmer et al., Phys. Lett. 122B, 41 (1983).
14. J. Bagger et al., Phys. Rev. Lett. 54, 2199 (1985).
15. W. Buchmüller and D. Wyler, Nucl. Phys. B268, 621 (1986).